

**The following resources related to this article are available online at [www.sciencemag.org](http://www.sciencemag.org) (this information is current as of July 14, 2009 ):**

**Updated information and services**, including high-resolution figures, can be found in the online version of this article at:

<http://www.sciencemag.org/cgi/content/full/309/5744/2228>

**Supporting Online Material** can be found at:

<http://www.sciencemag.org/cgi/content/full/309/5744/2228/DC1>

A list of selected additional articles on the Science Web sites **related to this article** can be found at:

<http://www.sciencemag.org/cgi/content/full/309/5744/2228#related-content>

This article **cites 32 articles**, 13 of which can be accessed for free:

<http://www.sciencemag.org/cgi/content/full/309/5744/2228#otherarticles>

This article has been **cited by** 48 article(s) on the ISI Web of Science.

This article has been **cited by** 24 articles hosted by HighWire Press; see:

<http://www.sciencemag.org/cgi/content/full/309/5744/2228#otherarticles>

This article appears in the following **subject collections**:

Neuroscience

<http://www.sciencemag.org/cgi/collection/neuroscience>

Information about obtaining **reprints** of this article or about obtaining **permission to reproduce this article** in whole or in part can be found at:

<http://www.sciencemag.org/about/permissions.dtl>

patients' lesions overlap (15). Our findings are similar to those obtained in nonhuman primates. Monkeys showed persistent signs of neglect after unilateral section of the white matter between the fundus of the intraparietal sulcus and the lateral ventricle (24). The greater effect of subcortical inactivation, as compared to cortical inactivation, is consistent with the idea that symmetrical space processing requires the integrity of a parietal-frontal network (1, 15). Damage to restricted regions of the white matter can cause the dysfunction of large-scale neurocognitive networks. According to an influential model (1), signs of left neglect result from impairment of a right-hemisphere network, including prefrontal, parietal, and cingulate components. The parietal component of the network could be especially important for the perceptual salience of extrapersonal objects, whereas the frontal component might be implicated in the production of an appropriate response to behaviorally relevant stimuli (1), in the online retention of spatial information (1, 25), or in the focusing of attention on salient items through reciprocal connections to more posterior regions (20).

Models of line bisection postulate a competition between the relative salience of the two lateral segments (6). The bisection mark is drawn at the point of subjective equality between the two segments (5). Bisection-related tasks activate the IPL in humans (26). Transcranial magnetic stimulation over the right posterior parietal cortex, but not over the STG, was found to bias the comparison of the lengths of the component segments of pretransected lines in a direction coherent with rightward shifts in line bisection (27). In the monkey, regions adjacent to the intraparietal sulcus, such as the lateral intraparietal area, are related to visual perceptual salience (11) and can reinforce the stimulus attentional priority (10). Parietal inactivation may thus bias the perceptual decision by modulating the salience of the line segments (6).

The assessment of spatial cognition during intraoperative stimulation offers the double opportunity of preserving spatial processing functions during brain surgery and of pinpointing the neurocognitive systems devoted to spatial processing in humans. Spatial awareness is dependent not only on the cortical areas of the temporal-parietal junction, but also on a larger parietal-frontal network communicating via the superior occipitofrontal fasciculus.

References and Notes

1. M. M. Mesulam, *Philos. Trans. R. Soc. London Ser. B* **354**, 1325 (1999).
2. P. Azouvi et al., *J. Neurol. Neurosurg. Psychiatry* **73**, 160 (2002).
3. P. Bartolomeo, S. Chokron, *Neurosci. Biobehav. Rev.* **26**, 217 (2002).
4. T. Schenkenberg, D. C. Bradford, E. T. Ajax, *Neurology* **30**, 509 (1980).
5. J. C. Marshall, P. W. Halligan, *Cognit. Neuropsychol.* **7**, 107 (1990).
6. B. Anderson, *Brain* **119**, 841 (1996).
7. G. Vallar, *Neuroimage* **14**, 552 (2001).
8. D. J. Mort et al., *Brain* **126**, 1986 (2003).

9. M. Corbetta, G. L. Shulman, *Nat. Rev. Neurosci.* **3**, 201 (2002).
10. J. W. Bisley, M. E. Goldberg, *Science* **299**, 81 (2003).
11. J. P. Gottlieb, M. Kusunoki, M. E. Goldberg, *Nature* **391**, 481 (1998).
12. H. O. Karnath, M. Fruhmann Berger, W. Kuker, C. Rorden, *Cereb. Cortex* **14**, 1164 (2004).
13. A. D. Milner, M. A. Goodale, *The Visual Brain in Action* (Oxford Univ. Press, Oxford, 1995).
14. H. O. Karnath, *Nat. Rev. Neurosci.* **2**, 568 (2001).
15. F. Doricchi, F. Tomaiuolo, *Neuroreport* **14**, 2239 (2003).
16. H. Duffau et al., *Brain* **128**, 797 (2005).
17. CAL and SB attended clinical observation because of epileptic seizures. They showed no abnormality on preoperative neurological and neuropsychological examination, consistent with the slowly infiltrative character of low-grade gliomas, whose clinical presentation rarely includes signs of focal brain disease other than epilepsy. In particular, there were no signs of neglect on paper-and-pencil tests (table S1). Intraoperative electrical stimulation was well tolerated, and the patients reported no abnormal visual sensations. They bisected horizontal lines with their left, dominant hand during brain surgery (28). Eight healthy left-handed subjects (mean age, 31 years; SD, 5.3; range, 26 to 38) served as controls. They performed 30 line bisections each, with the same test material and in a body position similar to that of the patients. Our patients' baseline performance was well within the range of the controls' performance (mean  $\pm$  SD,  $0.28 \pm 2.39$  mm) as well as that of 10 strongly left-handed normal individuals tested in another study (29) (mean  $\pm$  SD,  $-1.50 \pm 3.66$  mm). In an unselected population of 204 patients with right brain damage (2), 5 of the 10 patients with the strongest left-handedness deviated rightward on 20-cm lines as compared to controls (29), a frequency of impairment similar to that showed by right-handed patients (2).
18. M. Catani, R. J. Howard, S. Pajevic, D. K. Jones, *Neuroimage* **17**, 77 (2002).
19. The neurosurgeon stopped the resection after stimulation of the region labeled as 42 (Fig. 2A). As a consequence, region 42 corresponded to the deepest point on the floor of the rostral-superior part of the surgical cavity, and was thus easily identified on postoperative anatomical MRI scans. The white matter tract underlying region 42 was identified by overlapping the MRI scans with the DTI scans (fig. S1) (Fig. 2, C and D).
20. M. Petrides, D. N. Pandya, in *Principles of Frontal Lobe Function*, D. T. Stuss, R. T. Knight, Eds. (Oxford Univ. Press, Oxford, 2002), pp. 31–50.
21. The superior occipitofrontal fasciculus is a poorly known long association pathway. It terminates

rostrally in the lateral prefrontal cortex of the inferior and middle frontal gyri (18). Its caudal terminations are less known (18, 30), but despite its name, derived from early descriptions (31), the superior occipitofrontal fasciculus seems to terminate caudally in the superior parietal gyrus (18) and in the intraparietal sulcus [(30), p. 367].

22. We used line bisection because it is an easy task for patients to perform and allows repeated assessments in the time scale required by intraoperative testing. Bisection of centrally presented 20-cm lines correlates positively and significantly with cancellation tests and is a good predictor of clinical neglect as assessed by standardized scales (2, 28).
23. C. Rorden, M. Fruhmann Berger, H.-O. Karnath, *Cognit. Brain Res.*, published online 19 February 2005 (10.1016/j.cogbrainres.2004.10.022).
24. D. Gaffan, J. Hornak, *Brain* **120**, 1647 (1997).
25. M. Husain, C. Rorden, *Nat. Rev. Neurosci.* **4**, 26 (2003).
26. G. R. Fink, J. C. Marshall, P. H. Weiss, I. Toni, K. Zilles, *Neuropsychologia* **40**, 119 (2002).
27. A. Ellison, I. Schindler, L. L. Pattison, A. D. Milner, *Brain* **127**, 2307 (2004).
28. See supporting data on Science Online.
29. M. Rousseaux et al., *Rev. Neurol. (Paris)* **157**, 1385 (2001).
30. R. Nieuwenhuys, J. Voogd, C. van Huijzen, *The Human Central Nervous System: A Synopsis and Atlas* (Springer-Verlag, New York, 1988).
31. M. J. Déjerine, *Anatomie des Centres Nerveux* (Rueff, Paris, 1895).
32. J. R. Crawford, P. H. Garthwaite, *Neuropsychologia* **40**, 1196 (2002).
33. We thank the patients for their cooperation; P. Gatignol for help with intraoperative testing; J. Chiras and the Department of Neuroradiology of the Salpêtrière Hospital for MRI acquisitions; S. Kinkingnehun, C. Delmaire, J. B. Pochon, L. Thivard, and the staff of BrainVISA software for technical support for image analysis; and P. Azouvi and the members of the Groupe d'Etude sur la Rééducation et l'Evaluation de la Négligence (GEREN) for permission to use data from GEREN studies (2, 29).

Supporting Online Material

www.sciencemag.org/cgi/content/full/309/5744/2226/DC1  
 Materials and Methods  
 SOM Text  
 Tables S1 and S2  
 Figs. S1 and S2  
 References

17 June 2005; accepted 26 August 2005  
 10.1126/science.1116251

# Breakdown of Cortical Effective Connectivity During Sleep

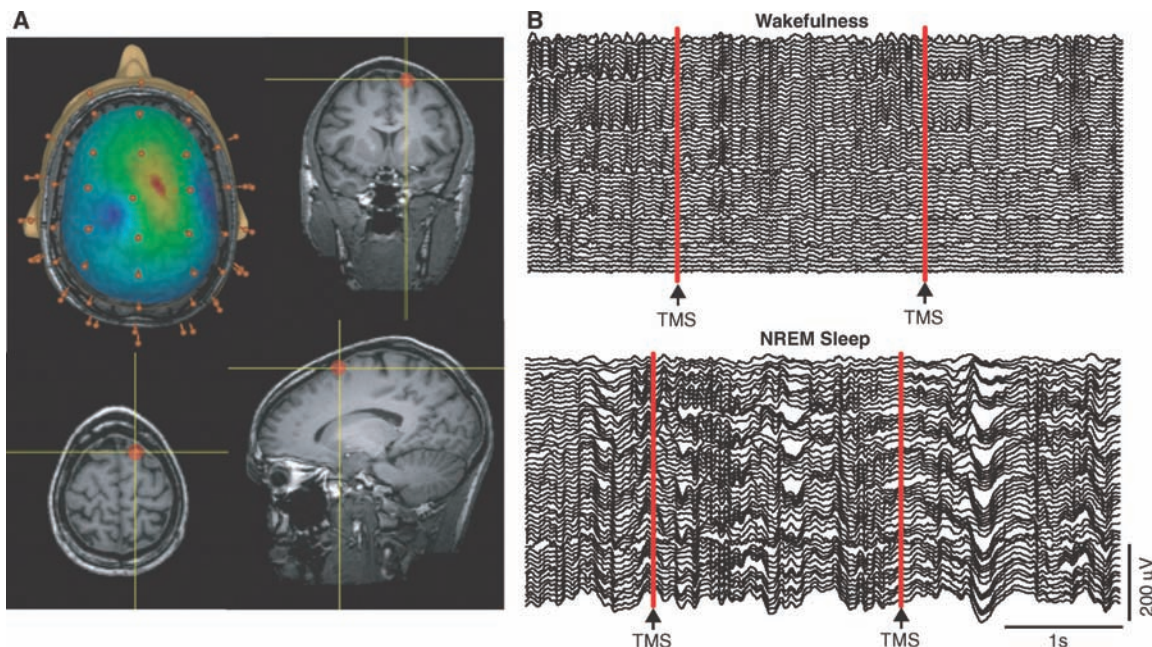
Marcello Massimini,<sup>1,2</sup> Fabio Ferrarelli,<sup>1</sup> Reto Huber,<sup>1</sup> Steve K. Esser,<sup>1</sup> Harpreet Singh,<sup>1</sup> Giulio Tononi<sup>1\*</sup>

When we fall asleep, consciousness fades yet the brain remains active. Why is this so? To investigate whether changes in cortical information transmission play a role, we used transcranial magnetic stimulation together with high-density electroencephalography and asked how the activation of one cortical area (the premotor area) is transmitted to the rest of the brain. During quiet wakefulness, an initial response (~15 milliseconds) at the stimulation site was followed by a sequence of waves that moved to connected cortical areas several centimeters away. During non-rapid eye movement sleep, the initial response was stronger but was rapidly extinguished and did not propagate beyond the stimulation site. Thus, the fading of consciousness during certain stages of sleep may be related to a breakdown in cortical effective connectivity.

When awakened early in the night from non-rapid eye movement (NREM) sleep, people often report little or no conscious experience

(1). It was first thought that this fading of consciousness was due to the brain shutting down. However, although brain metabolism is re-

**Fig. 1.** Navigated brain stimulation and EEG recordings during TMS. (A) The estimated electric field induced by TMS on the cortical surface in one subject is color-coded. The red area indicates the location of the maximal electric field strength (in this case, 81 V/m) and corresponds to the coordinates of the rostral premotor cortex, as identified on the three orthogonal projections of the subject's MRI. The brown pins represent the digitized electrodes. (B) Multichannel EEG recorded during wakefulness and NREM sleep while TMS (red) was delivered.



duced, the thalamocortical system remains active, with mean firing rates close to those that occur during quiet wakefulness (2). Moreover, coherent or synchronized activity continues to be detected among distant cortical areas (3–5), and sensory signals still reach the cerebral cortex (6). Why, then, does consciousness fade?

Recently we have proposed that consciousness depends critically not so much on firing rates, synchronization at specific frequency bands, or sensory input per se, but rather on the brain's ability to integrate information, which is contingent on the effective connectivity among functionally specialized regions of the thalamocortical system (7). Effective connectivity refers to the ability of a set of neuronal groups to causally affect the firing of other neuronal groups within a system (8). The fading of consciousness during NREM sleep episodes early in the night, evidenced by short or blank reports of cognitive activity upon awakening (1), would then be associated with an impairment of cortical effective connectivity.

To test this prediction, we used a combination of navigated transcranial magnetic stimulation (TMS) and high-density electroencephalography (HD-EEG) to measure the brain response to the direct perturbation of a chosen cortical region noninvasively and with good spatiotemporal resolution (9, 10). Using TMS/EEG to investigate critical differences in the functioning of the waking and sleeping brain offers several advantages. Unlike sensory stimulation, direct cortical

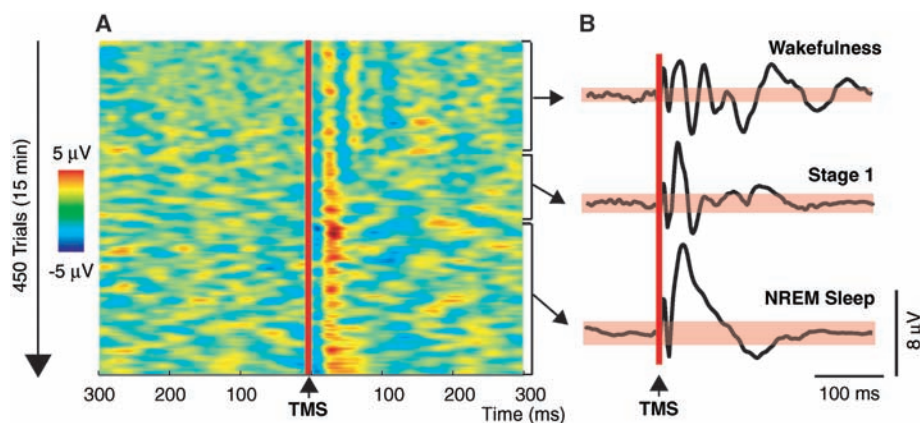


**Fig. 2.** Changes in the TMS-evoked response during shifts in the state of vigilance. (A) Single trials recorded from one channel located under the stimulator while the subject (the same as in Fig. 1) transitioned from wakefulness through stage 1 to NREM sleep. Single-trial EEG data (filtered from 4 to 100 Hz) are color-coded for voltage. (B) Averaged TMS-evoked responses (filtered from 1 to 100 Hz) obtained during the three states of vigilance. The horizontal pink bands indicate the significance level (3 SD from the mean prestimulus voltage).

stimulation does not activate the reticular formation and bypasses the thalamic gate. Thus, it directly probes the ability of cortical areas to interact, unconfounded by peripheral effects. Also, since study subjects reported that they were not aware of the TMS pulse, neural responses are not contaminated by reactions that may result from becoming aware of the stimulation. Most important, the combination of TMS and HD-EEG dissociates effective connectivity (causal interactions) from functional connectivity [temporal correlations (8)].

Using a 60-channel TMS-compatible EEG amplifier, we recorded TMS-evoked brain responses while six subjects, lying with eyes closed on a reclining chair, progressed from wakefulness to NREM sleep. By means of magnetic resonance image (MRI)-guided estimation

of the electric field induced on the surface of the brain (Fig. 1A), we targeted TMS to the rostral portion of the right premotor cortex. This is an area with extensive corticocortical connections that can be conveniently stimulated without eliciting muscle artifacts. Stimuli were delivered at random intervals (between 2 and 2.3 s) with intensity below the motor threshold (90%), resulting in a maximum electric field at the cortical target of between 75 and 84 V/m. We took special care to reduce the amount of auditory and somatosensory stimulation associated with each TMS pulse (11).

As shown in Fig. 1B, TMS did not interfere conspicuously with ongoing wake or sleep EEG patterns nor did it cause visible artifacts. However, TMS elicited a time-locked response that was visible on a single-trial basis

<sup>1</sup>Department of Psychiatry, University of Wisconsin, Madison, 6001 Research Park Boulevard, Madison, WI 53719, USA. <sup>2</sup>Department of Clinical Sciences, University of Milan, via G. B. Grassi 74, Milan 20157, Italy.

\*To whom correspondence should be addressed. E-mail: gtononi@wisc.edu

and that changed markedly from wakefulness to sleep. Figure 2A displays the single-trial responses recorded from one electrode located under the stimulator during a transition from wakefulness through stage 1 to NREM (stages 2 and 3) sleep (in the same subject as in Fig. 1). Figure 2B shows the averages calculated from the single trials collected in these three vigilance states. During wakefulness, TMS induced a sustained response made of recurrent waves of activity. Specifically, a sequence of time-locked high-frequency (20 to 35 Hz) oscillations occurred in the first 100 ms and was followed by a few slower (8 to 12 Hz) components that persisted until 300 ms. As soon as the subjects transitioned into stage 1 sleep, the TMS-evoked response grew stronger at early latencies but became shorter in duration: The amplitude of the initial components increased by 50 to 85% between 0 and 40 ms, whereas the subsequent waves were markedly dampened and fell below prestimulus noise levels (3 SD from the prestimulus baseline mean) within the first 150 to 200 ms. With the onset of NREM sleep, the brain response to TMS changed markedly. The initial wave doubled in amplitude and lasted longer. After this large wave, no further TMS-locked activity could be detected, except for a slight negative rebound between 80 and 140 ms. Specifically, fast waves, still visible during stage 1, were completely obliterated, and all TMS-evoked activity had ceased by 150 ms.

To better characterize the underlying neural events, we calculated the spatiotemporal dynamics of the currents induced by TMS in the cerebral cortex. We digitized and coregistered electrode positions to each subject's MRI, and we constructed a realistic head model. We then estimated current density on the cortical surface by using the weighted minimum norm least-squares method (11). Figure 3 shows the average responses recorded from all channels during wakefulness and NREM sleep in the same subject shown in Figs. 1 and 2. At early latencies, during both wakefulness and NREM sleep, TMS induced a clear dipolar voltage configuration that was centered under the coil and corresponded to maximum cortical activation in ipsilateral area 6. During wakefulness, this initial response was followed for about 300 ms by multiple waves of activity associated with rapidly changing configurations of scalp potentials. Current maxima shifted over time from the stimulation target to contralateral area 6, bilateral area 9, contralateral area 8, and ipsilateral area 7. The rostral premotor cortex has extensive transcallosal connections (12) and is linked to prefrontal areas (13). Thus, during wakefulness, the perturbation of the rostral premotor cortex was followed by spatially and temporally differentiated patterns of activation that appeared to propagate along its anatomical connections. In striking contrast, during NREM sleep the

location of maximum current density remained confined to the stimulated area.

As shown in Fig. 4, this breakdown in effective connectivity during sleep was evident and reproducible in all six subjects. We estimated current density whenever the global power of the evoked field was higher (>6 SD) than mean prestimulus levels and plotted the location of the strongest TMS-evoked activation on each subject's cortical surface, color-coded according to its latency (11). During wakefulness, the site of maximum activation moved back and forth among premotor and

prefrontal areas in both hemispheres and, in some subjects, it also involved the motor and posterior parietal cortex. During NREM sleep, by contrast, the activity evoked by TMS did not propagate in space and time in any of the subjects. In two subjects, we were also able to stimulate the parietal cortex (area 5), and we found a similar impairment of intracortical information transmission during NREM sleep (fig. S2). Thus, although TMS during sleep elicits an initial response that is even stronger than during wakefulness, this response remains localized, does not propagate to connected

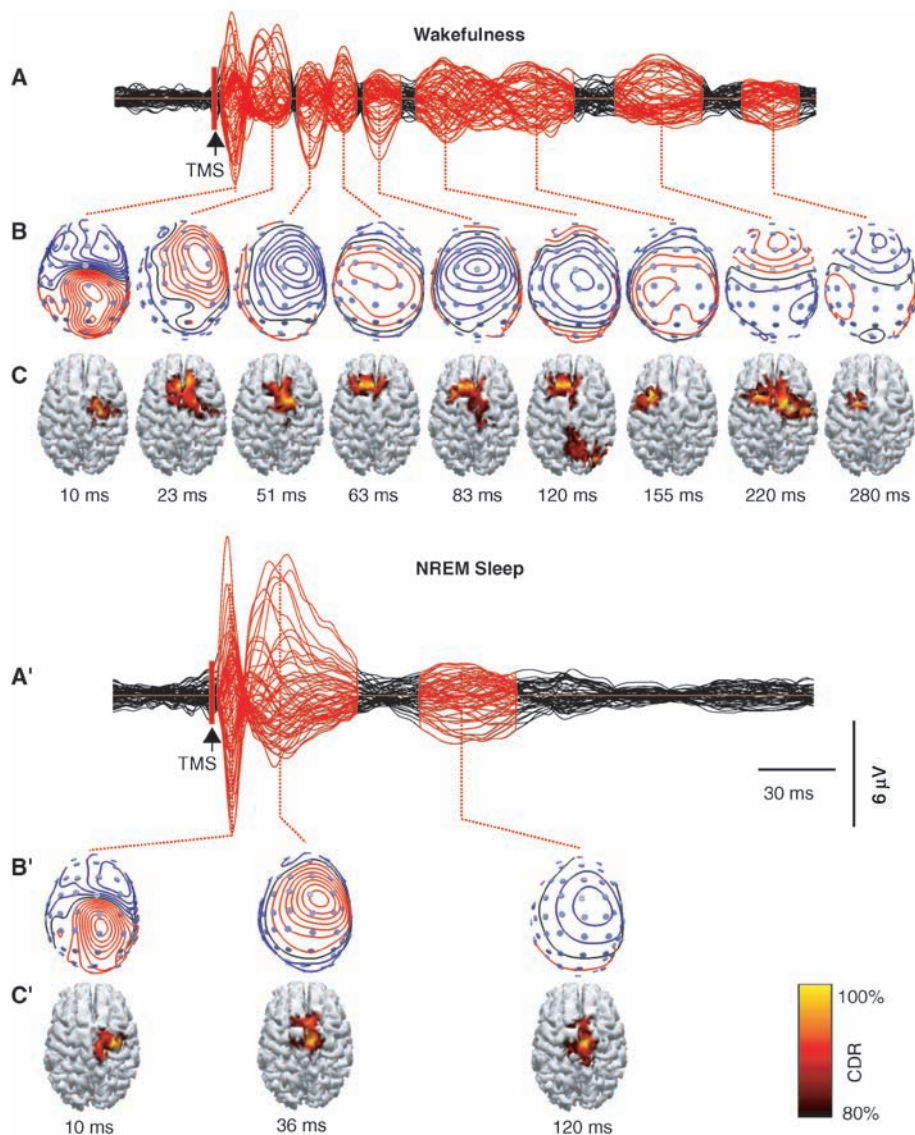


**Fig. 3.** Spatiotemporal dynamics of scalp voltages and cortical currents evoked by TMS during wakefulness and sleep. (A and A') Averaged TMS-evoked potentials recorded at all electrodes, superimposed in a butterfly diagram (black traces; the horizontal red line indicates the average reference), for the same subject as in Figs. 1 and 2. The time of TMS is marked by a vertical red bar. The red portions of the traces indicate the times at which TMS induced a significant response (see supporting online material for calculation details). Source modeling was performed at the local maxima of field power within periods of significant activity. (B and B') Three-dimensional contour voltage maps (red, positive; blue, negative; step = 0.6  $\mu\text{V}$  for wakefulness and 1  $\mu\text{V}$  for NREM sleep). (C and C') Corresponding current density distributions plotted on the cortical surface. At each time point, the results of the L2 Norm (see methods) were auto-scaled and thresholded at 80% to highlight maximum current sources (CDR, current density reconstruction).

brain regions, dissipates rapidly, lacks high-frequency components, and is stereotypical regardless of stimulation site.

Various mechanisms could account for the enhancement of early TMS-EEG responses in sleep, including a stronger driving force in hyperpolarized postsynaptic neurons (14), an increased discharge synchrony of cortical populations (15), a reduction in synaptic depression (16, 17), and thalamic bursting triggered by the TMS-induced corticothalamic volley (18). These mechanisms may also produce the enhancement of cortical components of visual, auditory, and somatosensory evoked potentials that has been reported during NREM sleep (6).

What causes the dramatic breakdown in cortical effective connectivity during sleep? During NREM sleep, cortical neurons are depolarized and fire tonically just as in quiet wakefulness, but these depolarized up-states are interrupted by short hyperpolarized down-states when neurons remain silent (19). The transition from up- to down-states appears to be due to depolarization-dependent potassium currents that increase with the amount of prior activation (19). Perhaps because of this bistability of cortical networks during NREM sleep (16, 17), any local activation, whether occurring spontaneously or induced by TMS, will eventually trigger a local down-state that prevents further propagation of activity. Al-

ternatively, the block may occur in the thalamus, whose neurons, when hyperpolarized, fire a single burst in response to corticothalamic volleys and then enter a prolonged inhibitory rebound (20). Finally, there may be sleep-related changes in the balance between excitation and inhibition (21), as suggested by paired-pulse TMS studies (22).

Whatever the precise mechanisms, they are most likely engaged by the progressive reduction of the firing of diffuse neuromodulatory systems that occurs when we fall asleep (23). Indeed, the blockade of intracortical signaling did not begin suddenly, and the spatiotemporal pattern of cortical activation during stage 1 sleep was intermediate between those of wakefulness and NREM sleep (fig. S3). Specifically, during stage 1 sleep, the TMS-evoked response propagated from the right premotor cortex to the homotopic contralateral site within the first few tens of milliseconds; however, this initial activation was not sustained nor did it reach prefrontal or parietal areas.

By using a combination of TMS and HD-EEG, we have found evidence for a breakdown of transcallosal and long-range effective connectivity during NREM sleep. This breakdown in the ability of cortical areas to interact effectively contrasts with the persistence or increase in interhemispheric and interareal broadband coherence that can be observed in

EEG studies of sleep (3, 24). Thus, an impairment in the ability to integrate information among specialized thalamocortical modules—a proposed theoretical requirement for consciousness (7)—may underlie the fading of consciousness in NREM sleep early in the night. It will be important to see whether cortical effective connectivity recovers in part during late-night sleep, especially during REM sleep, a time at which conscious reports become long and vivid (1). More generally, probing the brain's effective connectivity directly may prove useful in pharmacologically induced unconsciousness and in several psychiatric and neurological conditions in which consciousness is affected and neural interactivity may be compromised above and beyond neural activity and neural synchrony (25).

References and Notes

1. R. Stickgold, A. Malia, R. Fosse, R. Propper, J. A. Hobson, *Sleep* **24**, 171 (2001).
2. M. Steriade, I. Timofeev, F. Grenier, *J. Neurophysiol.* **85**, 1969 (2001).
3. P. Achermann, A. A. Borbely, *Neuroscience* **85**, 1195 (1998).
4. M. Steriade, D. A. McCormick, T. J. Sejnowski, *Science* **262**, 679 (1993).
5. Gamma activity and synchrony, which have been viewed as possible correlates of consciousness (26–28), were found to be low in NREM sleep in one study (29). However, they were equally low in REM sleep, when conscious experience is usually vivid, and they can be high during anesthesia (30). Moreover, intracellular recordings show that gamma activity persists during NREM sleep (31), and other studies report that gamma coherence is a local phenomenon that does not change between wakefulness and sleep (32). Large-scale synchrony in the alpha and theta bands may also correlate with conscious perception during wakefulness (33), but synchrony in these frequency bands actually increases during NREM sleep (3, 34).
6. R. Kakigi *et al.*, *Sleep Med.* **4**, 493 (2003).
7. G. Tononi, *BioMed Central Neurosci.* **5**, 42 (2004).
8. L. Lee, L. M. Harrison, A. Mechelli, *Neuroimage* **19**, 457 (2003).
9. R. J. Ilmonemi *et al.*, *Neuroreport* **8**, 3537 (1997).
10. A change in transcallosal responsiveness between wakefulness and sleep was observed in an experiment employing electrical stimulation of the corpus callosum and extracellular cortical recordings in monkeys [figure 8.19 in (35)]. Changes in TMS-evoked motor responses during sleep and after awakenings from different stages of sleep have also been reported (36, 37).
11. Materials and methods are available as supporting material on Science Online.
12. B. Marconi, A. Genovesio, S. Giannetti, M. Molinari, R. Caminiti, *Eur. J. Neurosci.* **18**, 775 (2003).
13. N. Picard, P. L. Strick, *Curr. Opin. Neurobiol.* **11**, 663 (2001).
14. R. N. Sachdev, F. F. Ebner, C. J. Wilson, *J. Neurophysiol.* **92**, 3511 (2004).
15. F. Worgotter *et al.*, *Nature* **396**, 165 (1998).
16. M. Bazhenov, I. Timofeev, M. Steriade, T. J. Sejnowski, *J. Neurosci.* **22**, 8691 (2002).
17. S. Hill, G. Tononi, *J. Neurophysiol.* **93**, 1671 (2005).
18. A. Destexhe, D. Contreras, M. Steriade, *J. Neurophysiol.* **79**, 999 (1998).
19. M. V. Sanchez-Vives, D. A. McCormick, *Nat. Neurosci.* **3**, 1027 (2000).
20. C. Pedroarena, R. Llinas, *Proc. Natl. Acad. Sci. U.S.A.* **94**, 724 (1997).
21. M. Steriade, J. Hobson, *Prog. Neurobiol.* **6**, 155 (1976).
22. F. Salih *et al.*, *J. Physiol.* **565**, 695 (2005).
23. M. Steriade, *Prog. Brain Res.* **145**, 179 (2004).
24. G. Dumermuth, D. Lehmann, *Eur. Neurol.* **20**, 429 (1981).

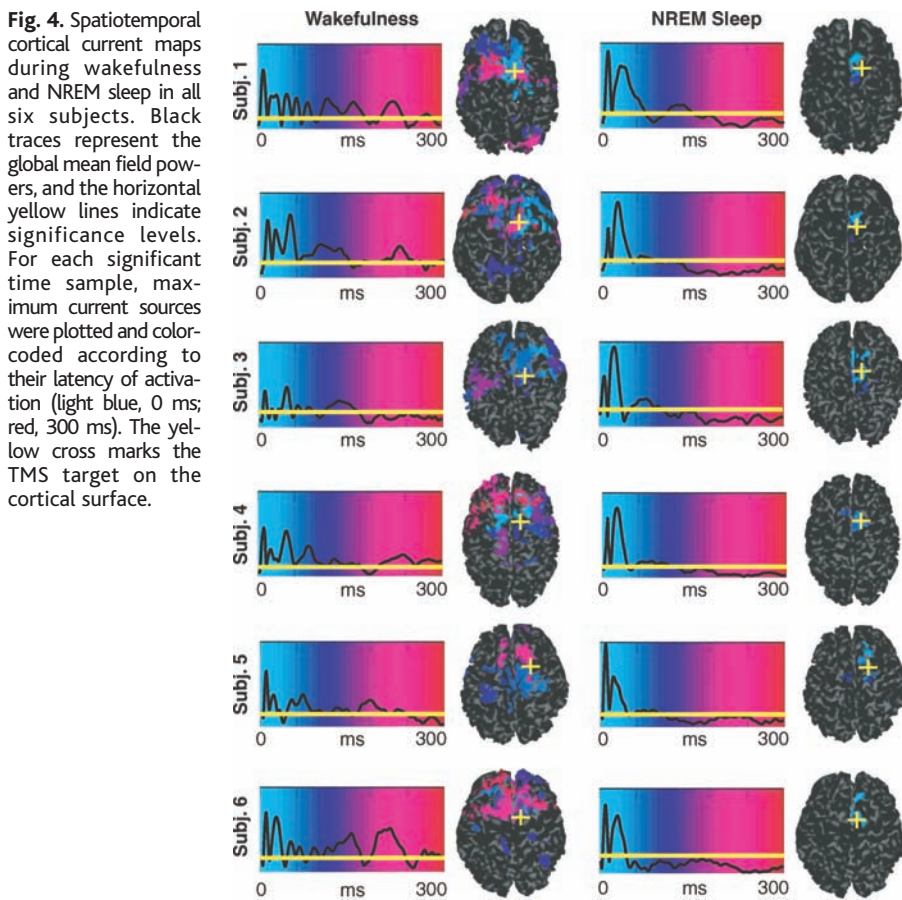


**Fig. 4.** Spatiotemporal cortical current maps during wakefulness and NREM sleep in all six subjects. Black traces represent the global mean field powers, and the horizontal yellow lines indicate significance levels. For each significant time sample, maximum current sources were plotted and color-coded according to their latency of activation (light blue, 0 ms; red, 300 ms). The yellow cross marks the TMS target on the cortical surface.

25. S. Laureys, A. M. Owen, N. D. Schiff, *Lancet Neurol.* **3**, 537 (2004).
26. F. Crick, C. Koch, *Cold Spring Harbor Symp. Quant. Biol.* **55**, 953 (1990).
27. R. Llinas, U. Ribary, D. Contreras, C. Pedroarena, *Philos. Trans. R. Soc. London Ser. B* **353**, 1841 (1998).
28. A. K. Engel, W. Singer, *Trends Cogn. Sci.* **5**, 16 (2001).
29. J. L. Cantero, M. A. Aizawa, J. R. Madsen, R. Stickgold, *Neuroimage* **22**, 1271 (2004).
30. C. H. Vanderwolf, *Brain Res.* **855**, 217 (2000).
31. M. Steriade, D. Contreras, F. Amzica, I. Timofeev, *J. Neurosci.* **16**, 2788 (1996).
32. T. H. Bullock *et al.*, *Proc. Natl. Acad. Sci. U.S.A.* **92**, 11568 (1995).
33. A. von Stein, C. Chiang, P. Konig, *Proc. Natl. Acad. Sci. U.S.A.* **97**, 14748 (2000).
34. R. B. Duckrow, H. P. Zaveri, *Clin. Neurophysiol.* **116**, 1088 (2005).
35. M. Steriade, M. Deschênes, P. Wyzinski, J. P. Hallé, in *Basic Sleep Mechanisms*, O. Petre-Quadens, J. Schlag, Eds. (Academic Press, New York, 1974), pp. 144–200.
36. M. Bertini *et al.*, *J. Sleep Res.* **13**, 31 (2004).
37. P. Grosse, R. Khatami, F. Salih, A. Kuhn, B. U. Meyer, *Neurology* **59**, 1988 (2002).
38. We thank A. Alexander, C. Cirelli, S. Hill, and B.

Riedner for their help. Supported by the National Sleep Foundation (Pickwick Fellowship) and by the National Alliance for Schizophrenia and Depression.

#### Supporting Online Material

www.sciencemag.org/cgi/content/full/309/5744/2228/DC1

Materials and Methods

Figs. S1 to S3

References and Notes

11 July 2005; accepted 29 August 2005

10.1126/science.1117256

## IP<sub>3</sub> Receptor Types 2 and 3 Mediate Exocrine Secretion Underlying Energy Metabolism

Akira Futatsugi,<sup>1,2\*</sup> Takeshi Nakamura,<sup>1,3</sup> Maki K. Yamada,<sup>3</sup> Etsuko Ebisui,<sup>1,2</sup> Kyoko Nakamura,<sup>1,3</sup> Keiko Uchida,<sup>3</sup> Tetsuya Kitaguchi,<sup>2</sup> Hiromi Takahashi-Iwanaga,<sup>4</sup> Tetsuo Noda,<sup>5</sup> Jun Aruga,<sup>2</sup> Katsuhiko Mikoshiba<sup>1,2,3\*</sup>

Type 2 and type 3 inositol 1,4,5-trisphosphate receptors (IP<sub>3</sub>R2 and IP<sub>3</sub>R3) are intracellular calcium-release channels whose physiological roles are unknown. We show exocrine dysfunction in IP<sub>3</sub>R2 and IP<sub>3</sub>R3 double knock-out mice, which caused difficulties in nutrient digestion. Severely impaired calcium signaling in acinar cells of the salivary glands and the pancreas in the double mutants ascribed the secretion deficits to a lack of intracellular calcium release. Despite a normal caloric intake, the double mutants were hypoglycemic and lean. These results reveal IP<sub>3</sub>R2 and IP<sub>3</sub>R3 as key molecules in exocrine physiology underlying energy metabolism and animal growth.

Inositol 1,4,5-trisphosphate receptors (IP<sub>3</sub>Rs) are intracellular Ca<sup>2+</sup> release channels located on the endoplasmic reticulum (ER) that mediate Ca<sup>2+</sup> mobilization from the ER to the cytoplasm in response to the binding of a second messenger, inositol 1,4,5-trisphosphate (IP<sub>3</sub>) (1). IP<sub>3</sub>-induced Ca<sup>2+</sup> release is triggered by various external stimuli, and most non-excitabile cells use this mechanism as the primary Ca<sup>2+</sup> signaling pathway. IP<sub>3</sub>Rs are therefore thought to have important physiological roles in various cell types and tissues (2). Three subtypes of IP<sub>3</sub>Rs, derived from three distinct genes, have been identified in mammals (3). Type 1 IP<sub>3</sub>R (IP<sub>3</sub>R1) is predominantly expressed in brain tissue and plays a critical role in the regulation of motor and learning

systems (4–7). The other two subtypes, type 2 and 3 IP<sub>3</sub>Rs (IP<sub>3</sub>R2 and IP<sub>3</sub>R3), are expressed in various tissues and cell lines (8–11); however, the importance of these subtypes in vivo has been difficult to assess because of their co-expression in tissues and the lack of selective inhibitors. In this study, we examined mice lacking both IP<sub>3</sub>R2 and IP<sub>3</sub>R3 and observed defects in the digestive system resulting from the lack of Ca<sup>2+</sup> signaling in exocrine tissues. In such exocrine tissues, secretagogue-induced increases in intracellular Ca<sup>2+</sup> concentration ([Ca<sup>2+</sup>]<sub>i</sub>) trigger the secretion of enzymes or water by acting on the Ca<sup>2+</sup>-dependent exocytotic machinery or ion channels, respectively (12–16). A crucial physiological role of IP<sub>3</sub>Rs in exocrine Ca<sup>2+</sup> signaling was demonstrated (15, 17); however, the relative importance of the three different IP<sub>3</sub>R subtypes has been unclear.

We generated mice lacking either IP<sub>3</sub>R2 or IP<sub>3</sub>R3 by disrupting the corresponding genes within their first coding exons (figs. S1A and S1B). The single-gene mutants were viable and showed no distinct abnormalities in appearance, at least for several months after birth. Mutant mice lacking both of these IP<sub>3</sub>R subtypes were also viable during the embryonic period. Immunoblot analysis of the submandibular glands and the pancreas, where IP<sub>3</sub>R2 and IP<sub>3</sub>R3 are expressed (fig. S1C),

showed that expression of IP<sub>3</sub>R2 and IP<sub>3</sub>R3 was abolished in the mutants (Fig. 1A). At birth, the appearance of double homozygotes was indistinguishable from that of nonhomozygous littermates, but double homozygotes had gained less body weight after birth. After the weaning period, around postnatal day 20 (P20), the homozygotes began losing weight and died within the 4th week of age (Fig. 1B). We suspected that an incapability of the double mutants to eat dry food after weaning might have caused body weight loss and eventual death. Indeed, double mutants did not consume dry food at all. When the double mutants were fed wet mash food beginning at P20, they consumed this type of food and survived thereafter. Body weight increases of the double mutants, however, were still smaller than those of nondouble mutant littermates equally fed with wet mash food (Fig. 1C). Interestingly, despite their reduced body weights, the double mutants consumed no less wet mash food than did the control mice (Fig. 2A and fig. S2A). The double mutants also took as much milk as did control mice when they were fed milk instead of wet mash food after weaning (fig. S2B). Thus, the caloric intake of the IP<sub>3</sub>R2<sup>-/-</sup>-IP<sub>3</sub>R3<sup>-/-</sup> double mutants appeared to be slightly greater than that of the control mice. In addition, the amount of feces produced by adult mice fed wet mash food was higher in the double mutants (Fig. 2B). The total amount of proteins and lipids in the feces were higher in the double mutants (Fig. 2C and fig. S2C). Furthermore, blood glucose concentrations were significantly lower in the double mutants (86.1 ± 5.3 mg/dl, *n* = 11) than those in control mice (156.1 ± 6.5 mg/dl, *n* = 14). Altogether, these results suggest that digestive system dysfunction causes the malnutrition phenotype of the double mutants. Actually, when the double mutants were fed a predigested diet containing glucose and amino acids for a week, they gained weight (1.7 ± 0.7 g, *n* = 8), whereas those fed wet mash food did not (-0.5 ± 0.3 g, *n* = 5).

Because the lethal double mutant phenotype was partially rescued by macerating the food with water, we hypothesized that the double mutants might be deficient in saliva production. We therefore examined saliva secretion in adult mice stimulated by subcutaneous

<sup>1</sup>Calcium Oscillation, International Cooperative Research Project, Japan Science and Technology Agency, Tokyo 108-0071, Japan. <sup>2</sup>Laboratory for Developmental Neurobiology, Brain Development Research Group, Brain Science Institute, RIKEN, Saitama 351-0198, Japan. <sup>3</sup>Division of Molecular Neurobiology, Institute of Medical Science, University of Tokyo, Tokyo 108-8639, Japan. <sup>4</sup>Department of Anatomy, School of Medicine, Hokkaido University, Sapporo 060-8638, Japan. <sup>5</sup>Department of Cell Biology, Japanese Foundation for Cancer Research, Cancer Institute, Tokyo 170-8455, Japan.

\*To whom correspondence should be addressed. E-mail: afutatsu@brain.riken.jp (A.F.); mikoshiba@ims.u-tokyo.ac.jp (K.M.)